Scientific Research Publishing

Journal of Modern Physics, 2024, 15, 596-612
https://www.scirp.org/journal/jmp
ISSN Online: 2153-120X
ISSN Print: 2153-1196

Dark Matter Particles May Never Be Directly Detected by Instruments—A Dark Matter Mechanism That Does Not Exceed the Standard Model Framework

Wenbing Qiu

Key Laboratory of Ecophysics and Department of Physics, College of Science, Shihezi University, Shihezi, China
Email: 2962546794@qq.com

How to cite this paper: Qiu, W.B. (2024) Dark Matter Particles May Never Be Directly Detected by Instruments—A Dark Matter Mechanism That Does Not Exceed the Standard Model Framework. *Journal of Modern Physics*, **15**, 596-612.
https://doi.org/10.4236/jmp.2024.155028

Received: February 21, 2024
Accepted: April 14, 2024
Published: April 17, 2024

Abstract

A dark matter mechanism within the framework of the standard model (SM) of particle physics is proposed in this article that the essence of dark matter may be the excited virtual particle field by the gravitational field of ordinary matter, which contains virtual photons, virtual positive and negative electron pairs, virtual gluons, virtual positive and negative quark pairs, virtual neutrinos etc. In this mechanism, there are two basic assumptions: 1) the stronger the gravitational field of ordinary matter, the greater the excited energy (mass) density of virtual particle field; 2) The excited virtual particle field is generally very weak in self-interaction. The virtual particle field excited by gravity can exhibit the properties of dark matter and may become a dark matter candidate. Based on this new dark matter mechanism, the hydrodynamic equations and cosmic perturbation equations describing cosmic matter are improved, and this may be meaningful for solving the challenges faced by the standard cosmological model (Lambda-CDM or LCDM) and developing and perfecting LCDM model.

Keywords

Dark Matter, Virtual Particle, Gravitational Field, Ordinary Matter

1. Introduction

"Dark matter" has always been one of the big problems to be solved in physics. Astronomers found that the observed galaxy velocity can't be explained by the Newton's dynamics theory, and more gravitational sources are needed. So, they

proposed to introduce "invisible" dark matter. The concept of dark matter is supported by a large number of astronomical and cosmological observations such as galaxy rotation curve, gravitational lens effect, bullet galaxy cluster, cosmic large scale structural and microwave background radiation etc. But after decades of searching, people have not found any dark matter particles. So, what on earth is the essence of dark matter? So far, it is still not clear, but it can be determined that there are the following properties for dark matter:

(1) Dark matter is or almost is electrically neutral and chromatically neutral (No SU (3) color charge);

(2) Dark matter is very stable (it has been existing since the Big Bang);

(3) Dark matter is cold or warm, *i.e.* nonrelativistic or at least not ultra-relativistic;

(4) Dark matter does interact via gravity.

There are many particle models to explain the essence of dark matter. The most popular is the cold dark matter (CDM) or LCDM model, which is mainly based on super standard model particles such as Weakly Interacting Massive Particle, axion, neutralino, etc. But, the LCDM model faces a number of challenges [1] [2], among which Hubble constant crisis and small-scale difficulties (the cusp-core problem, the missing satellite problem and the too-big-to-fail problem etc.) are the most studied. Thus far, these problems are not still really or thoroughly solved although many solutions, such as considering baryonic physics, warm dark matter (WDM), self-interacting dark matter (SIDM) and modifying the early-time universe [3] etc., have been proposed. None of these solutions takes the small-scale difficulty and Hubble constant crisis into account together, only being able to deal with one of the two.

In this article, a new dark matter mechanism is put forward, bringing the small-scale difficulties and Hubble constant crisis into a unified processing framework.

It is thought in this article that the small-scale difficulties may indicate that our current understanding of the essence of dark matter or CDM is still biased, whereas this may also result in the Hubble constant crisis. That is to say, the small-scale difficulties and Hubble constant crisis may stem from the same reason. Thereby, the theory about the essence of dark matter or CDM still needs to be further explored. It is thought in common conception that no SM particle accords with all properties of dark matter, but it is found in this paper that a possible dark matter mechanism can be suggested under the category of SM, which provides a new idea for understanding dark matter essence and solving the problems faced by LCDM.

This article is organized as follows: Section 2 is the main body of this paper. A new dark matter mechanism is explained in Section 2. In Section 3, the improvements of cosmic hydrodynamic equations and cosmic perturbation equations are discussed, respectively. The summary of this paper is concluded in Section 4.

The natural unit system is adopted in this article.

2. Virtual Particle Field Excited by Gravitation May Become Dark Matter

People's cognition that SM particles can't satisfy the properties of dark matter is based on the concept of "real particles" (which can be directly detected by instruments) in quantum field theory. If we consider virtual particles (which cannot be directly detected by instruments), SM particles may also become candidates for dark matter. The analysis is as follows:

(1) The gravitational field of ordinary matter excites the virtual particle field.

According to quantum field theory and general relativity, vacuum is the ground-state quantum field with minimum energy $\rho_{vac} = \Lambda/(8\pi G) \sim 10^{-7}\,\mathrm{GeV/cm^3}$ [4] (vacuum energy density), where Λ and G are the cosmological constant and gravitational constant, respectively. Vacuum is not empty, filled with various virtual particles such as virtual photons, virtual positive and negative electron pairs, virtual gluons, virtual positive and negative quark pairs, virtual neutrinos etc (Of course, the inclusion of virtual particles beyond SM is not excluded). These virtual particles are constantly generated and annihilated, known as "vacuum fluctuation". Vacuum is a self-acting mixture and it presents electrical neutrality and color neutrality.

Since vacuum has energy (mass), vacuum also participates in gravity. Just as charge can excite electrostatic field (the excited virtual photon field with higher energy density) from vacuum, celestial bodies (such as galaxy, galaxy cluster etc) of ordinary matter can also excite vacuum through their own gravity, thus generating virtual particle field with higher energy density $\rho_{exc} > \rho_{vac}$.

Here it is assumed that

① the stronger the gravitational field strength E_{LM} of ordinary matter, the greater the energy density ρ_{exc} of the excited virtual particle field (EVPF). Moreover, for the given matter distribution (for instance, gas, galaxy, galaxy cluster etc), there is a quantitative relationship between ρ_{exc} and E_{LM}

$$\Delta\rho = \rho_{exc} - \rho_{vac} = \ell\left(E_{LM}\right)^{\eta}, \tag{1}$$

where ℓ and η are two undetermined positive real parameters, the values of which are assumed to be related to and determined by the shape, size, sparseness and denseness of mass distribution (This assumption means that different mass distributions correspond to different the values of ℓ and η).

② The self-interaction of EVPF is very weak, except in the case of very strong gravitational field, such as galactic center and very early universe etc.

(2) EVPF shows the properties of dark matter

According to the above, one can infer that

① The electrical neutrality and color neutrality of EVPF. Unlike electrostatic field, which can respectively exert force in opposite directions on the positive and negative particles (charges) in a virtual particle pair, thus causing relative displacement of positive and negative particles and vacuum polarization, gravitational field exerts force in the same direction on the positive and negative par-

ticles in a virtual particle pair, thus not causing relative displacement of positive and negative particles and vacuum polarization. So, EVPF is electrically neutral and color neutral.

② The stability of EVPF.EVPF has always existed since the Big Bang, because ordinary matter has always existed, and its gravitation always excites virtual particle field.

③ According to the assumption ② in the above analysis (1), EVPF can generally be regarded as a collisionless and pressureless particle field or ideal fluid, which is described by the Boltzmann equation or hydrodynamic equations.

④ EVPF interacts via gravity, because it has mass.

⑤ EVPF is cold. The structure of the universe comes from the small fluctuation (perturbation) of the early universe. Because of the randomness of the fluctuation, it is assumed that the velocity of baryon, including neutrino, is approximately equiprobable in all directions, thus the average velocity of large number of baryons is zero or very small. So, the overall movement (large number of baryons' average velocity) of baryon matter such as nebula gas in the late universe, baryonic plasma in the early universe etc, which is made up of large number of baryons, is non-relativistic.

According to the hypothesis ① in the above analysis (1), EVPF mainly tracks the strong gravitational field, whereas the strong gravitational field tracks the high-density ordinary matter. So, EVPF tracks mainly the high-density ordinary matter (baryon matter).As just stated in the previous paragraph, the motion of baryon matter is non-relativistic, so the EVPF tracking baryon matter is also non-relativistic (cold).

⑥ EVPF, as the cold ideal fluid, is described by the Boltzmann equation (Temporarily disregarding the impact of Equation (1)), and it can naturally describe and explain the formation of cosmic large-scale structure.

⑦ EVPF, as the cold fluid, is described by cosmic perturbation equations (Temporarily disregarding the impact of Equation (1)), and it can naturally describe and explain the anisotropy and angular power spectrum of cosmic microwave background (CMB).

⑧ EVPF can explain the bullet cluster.

The EVPF can explain why dark matter does not trace the cluster gas which contains the main mass component of the merging cluster in the bullet galaxy cluster. According to the above, EVPF tracks mainly the high-density ordinary matter. In the bullet cluster, the high-density ordinary matter is obviously the galaxy, not gas. Although the mass of gas is much larger than that of galaxies, its density distribution is very small compared with galaxies. Thereby, in the bullet cluster EVPF tracks mainly the galaxies. In addition, due to the electrical neutrality of EVPF, it is not subjected to electromagnetic blockade by gases. So, finally EVPF is separated from gas.

⑨ EVPF can explain the characteristics of the cosmic map of dark matter (See Figure 1).

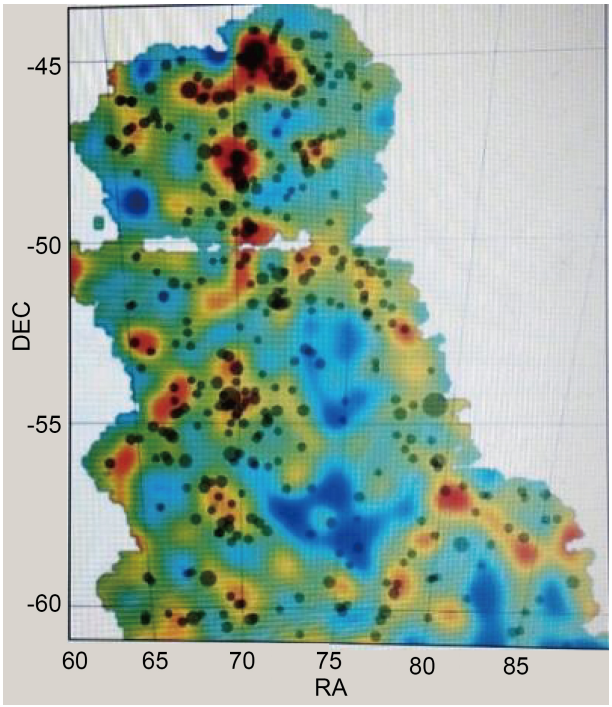

Figure 1. The red areas represent the highest concentrations of dark matter, the orange and yellow the next highest. The blue areas are voids where low densities of dark matter and clusters of galaxies are found. The existence of dark matter filamentary structures in the red, orange, and yellow colors is clearly manifested. The gray dots represent galaxy clusters, and the bigger the dot, the larger the cluster. The data come from [5].

The characteristics of this map are that the dark matter always envelops galaxies and clusters of galaxies, and the clusters are preferentially found in the dark matter areas, and orange and yellow filament structures. They are scarcely found in the blue voids. The explanation for this distribution characteristic is that EVPF follows the high-density ordinary matter (galaxy, galaxy cluster).

⑩ EVPF can explain galaxy rotation curve

Here, the Milky Way (MW), as a stable system with invariant mass distribution and constant parameter values (ℓ and η), is taken as an example. The baryon matter of MW is bulge and disk.

The gravitational field of the bulge is assumed to be depicted by the Plummer potential [6]

$$\varphi_b(R) = -GM_b \Big/ \sqrt{R^2 + z^2 + b_0^2}\,. \tag{2}$$

where $R = \left(x^2 + y^2\right)^{1/2}$. M_b and b_0 are the bulge mass and scale constant, respectively, the values of which are directly taken from [6].

For the MW disk, the sum of three MN potentials is adopted [7]

$$\varphi_d(r,z) = -\sum_{i=1}^{3} GM_{d,i} \Big/ \sqrt{r^2 + \left(a_i + \sqrt{z^2 + b_i^2}\right)^2}\,. \tag{3}$$

Here $M_{d,i}, a_i$ and b_i are the mass, radial scale length and vertical scale height of the disk, respectively, the values of which are directly taken from [7].

Thereby, the gravitational field strength produced by baryon matter (BM) is

$$E_{BM}(R,z)=\sqrt{\left(E_R^{bulge}(R,z)+E_R^{disk}(R,z)\right)^2+\left(E_z^{bulge}(R,z)+E_z^{disk}(R,z)\right)^2}.$$

where $E_j^k(R,z)=-\partial_j\varphi^k, k=1,2$ represents the bulge and disk, respectively; whereas $j=1,2$ represents the cylindrical coordinate R and z, respectively.

According to (1), the mass density of EVPF (dark matter or DM) excited by the gravitational field of the baryon matter of MW can be obtained

$$\rho_{DM}(R,z)=\ell\left[E_{BM}(R,z)\right]^{\eta}+\rho_{vac}\approx\ell\left[E_{BM}(R,z)\right]^{\eta}. \tag{4}$$

This approximation is based on $\rho_{DM}\gg\rho_{vac}$ at small scale.

Thus, the total mass of dark matter within the radius R range is

$$M_h(R)=\int_0^R\Sigma_{DM}(R')\times 2\pi R'\mathrm{d}R'. \tag{5}$$

Here $\Sigma_{DM}(R)=\int_{-\infty}^{\infty}\rho_{DM}(R,z)\mathrm{d}z$ is the surface mass density of dark matter projected along the z axis.

The circular velocity of dark matter contribution is thus obtained by

$$V_h(R)=\sqrt{GM_h(R)/R}.$$

The rotational velocity contributed by each component of baryon matter can be obtained from the corresponding gravitational field strength of each component

$$V_k(R)=\sqrt{R\times E_R^k(R,z=0)}.$$

So, the total circular velocity of MW is finally obtained

$$V_c(R)=\sqrt{V_{bulge}^2(R)+V_{disk}^2(R)+V_h^2(R)}. \tag{6}$$

Equation (6) is a rotation curve model with two parameters ℓ and η, used to fit the observed data of MW (See **Figure 2** below).

Based on the fit parameters in **Figure 2**, the distribution of dark matter of MW can be discussed (See **Figures 3-5** below).

It can be seen from **Figure 3** that the density distribution of dark matter is ellipsoidal. The axial ratios of dark matter halo gradually decreases from outside to inside. In the outer region, the shape is closer to sphericity, while in inner region, the shape deviates more significantly from sphericity. The nonsphericity of dark matter halo has long since been revealed in some work [9] [10]. What's more, it has been also pointed out in reference [10] that the shape (axis ratio) of dark halo varies at different radii and the nonsphericity of dark matter halo might help to resolve the "cusp-core problem" of dark matter halo.

From **Figure 3** and **Figure 4**, it can also be seen that the density values of the dark matter halo with ellipsoid-shape are different from those [11] of the dark matter halo based on spherical symmetry assumption, especially in the central region of the galaxy. It can be inferred that when the gravity field in the inner region or the central region deviates greatly from spherical symmetry, the dark

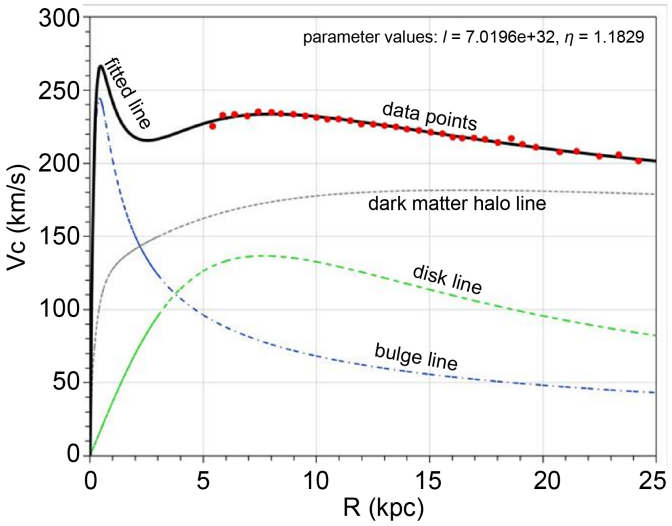

Figure 2. Fitting diagram of two-parameter rotation curve for MW with $u_r = 0.0078$. Here u_r is called "standard relative error", defined by $u_r = \sqrt{\frac{\sum_{i=1}^{n}\left[\left(V_c(R_i) - V_{obs}(R_i)\right)/V_{obs}(R_i)\right]^2}{n}}$. Where $V_{obs}(R_i)$ is the observed velocity at radius R_i, n is the number of data points. Data points are taken from [8]. The values of ℓ and η are searched by using least square method, based on the mass unit of $10^9 M_\Theta$ (M_Θ is the mass of Sun) and the length unit of 1 kpc.

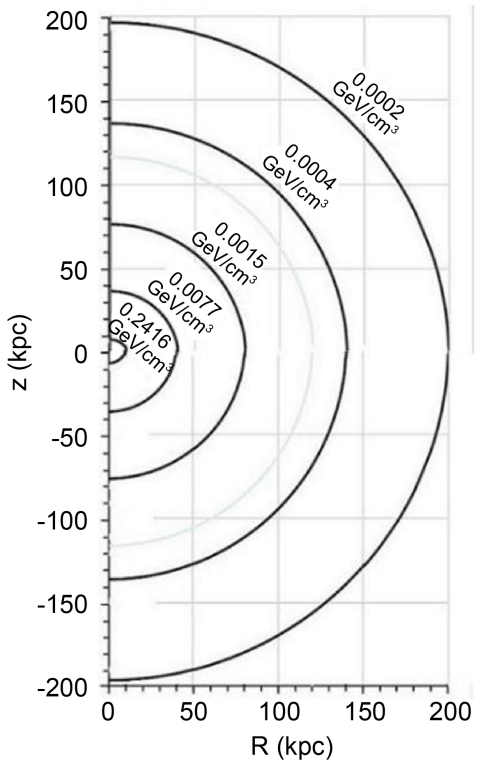

Figure 3. The isodensity line (surface) of dark matter halo calculated by (4).

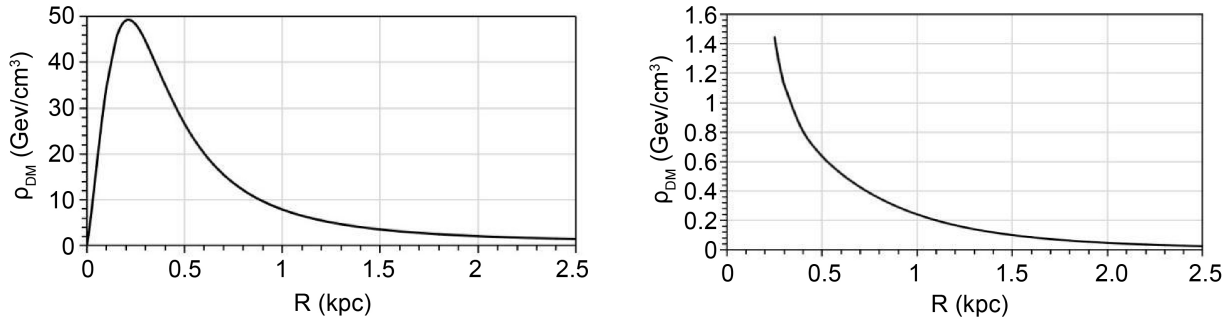

Figure 4. The radial distribution of dark matter halo density in the galactic plane (z = 0) based on the dual parameter model in **Figure 2**. *Left*: the profile within the bulge. *Right*: the profile outside the bulge. There is no cusp-core in the center of MW.

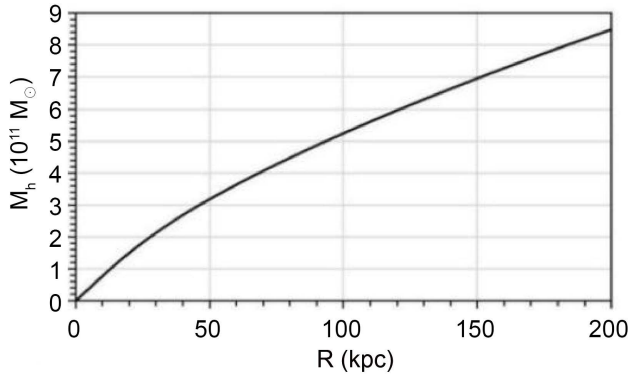

Figure 5. Function diagram of dark matter halo mass changing along the galactic plane radius based on the dual parameter model in **Figure 2**. The halo mass is computed by using (5). It can be seen that $M_h > 8\times10^{11}M_\odot$ when $R > 190$ kpc.

matter density difference between the two models will be also large, and the dark matter density profile in the inner region or the central region will deviate greatly from the familiar shape (for example for the dwarf galaxy, the familiar central profile of dark matter is the flat straight line. This flat straight profile also comes from the spherical symmetry assumption of dark halo [12]. If there is a great deviation from spherical symmetry in central region, dark halo density has also a great deviation from the flat straight profile).

⑪ EVPF can explain gravitational lens effect

Here, the famous gravitational lens system "cosmoic horseshoe" (SDSS J1004 + 4112) will be discussed, in which the lens is regarded as a stable celestial body with invariant mass distribution and constant ℓ and η. The parameter information of SDSS J1004 + 4112 can be viewed in [13] [14]. Tiny Tim 2 (Krist *et al.* 2011) [15] is used to obtain a model for the point-spread function (PSF).

To simulate the observed image, the lens model is constructed below.

For the foreground elliptical galaxy (lens), the gravitational potential of baryon matter is set to

$$\varphi_{BM}(x,y,z) = \alpha\left(\sqrt{x^2+qy^2+z^2}\right)^{\beta}. \tag{7}$$

Here $\alpha < 0$, $q > 1$ and $-2 < \beta < 0$ are three undetermined parameters.

Thus, the gravitational field strength and mass density of baryon matter can be derived out from (7)

$$\begin{aligned} E_{BM} &= \sqrt{\left(-\partial_x \varphi_{BM}\right)^2 + \left(-\partial_y \varphi_{BM}\right)^2 + \left(-\partial_z \varphi_{BM}\right)^2} \\ &= \alpha\beta\left(x^2 + qy^2 + z^2\right)^{\frac{\beta-2}{2}} \sqrt{x^2 + q^2 y^2 + z^2}, \end{aligned} \tag{8}$$

$$\begin{aligned} \rho_{BM} = \frac{1}{4\pi G}\nabla^2 \varphi_{BM} = \frac{1}{4\pi G}\alpha n\left(x^2 + qy^2 + z^2\right)^{\frac{\beta}{2}-2} \\ \times\left[\left(\beta + q\right)x^2 + \left(2 + \beta q - q\right)qy^2 + \left(\beta + q\right)z^2\right]. \end{aligned} \tag{9}$$

From (8), the dark matter density can be obtained $\rho_{DM} = \ell \cdot E_{BM}^{\eta}$.

Finally, the dimensionless surface mass density of the lens is given by

$$\kappa\left(x, y\right) = \Sigma\left(x, y\right)/\Sigma_{cr}. \tag{10}$$

where Σ_{cr} is the critical surface mass density, which can be calculated by the use of the data in [13].

$$\Sigma\left(x, y\right) = \int_{-\infty}^{\infty}\left[\rho_{BM}\left(x, y, z\right) + \rho_{DM}\left(x, y, z\right)\right]\mathrm{d}z. \tag{11}$$

is the total surface mass density for the lens, which includes the contribution of baryon matter and that of dark matter.

Equation (10) is a 5-parameter lens mass model.

An external shear component $\gamma = \left(\gamma_1, \gamma_2\right)$ is added to the lens model to describe the contribution from the mass distribution outside the main lens. γ_1 is aligned with the image's x-axis, while γ_2 is rotated by 45˚ counter-clockwise.

For depicting the light distributions of foreground and background galaxies, one Sérsic model and five Sérsic models (The Sérsic parameters of all models are $n = 4$) are adopted, respectively.

In specific numerical simulation, the shear components $\gamma_1 = 0.0539$, $\gamma_2 = -0.0192$ and the position angle (This angle indicates the direction of the major axis of the elliptical lens, measured east of north) $\varphi = 23.4$ are directly taken from [14]. The fitting results are shown in **Table 1** and **Figure 6** after using matlab fminsearch function to minimize the objective function

$$\chi^2 = \frac{1}{N+1}\left\{\sum_{i=1}^{N}\left[\left(I_i^{obs} - I_i^{sim}\right)^2/\sigma_i^2\right] + \left(M_0 - M\right)^2/\sigma_0^2\right\}.$$

where i presents the i-th pixel of the image. N presents the total number of pixels. I_i^{obs}, I_i^{sim} and σ_i are the observed brightness, mock brightness and the error of the observed brightness at the i-th pixel, respectively. I_i^{sim} is smoothed with the PSF of the observation. M and M_0 represent the closed masses of the Einstein ring for the model in this paper and the model in reference [13], respectively. σ_0 is the error of M_0. The values of M_0 and σ_0 are taken from [13].

It can be seen from **Table 1** that the foreground elliptical galaxy (lens) and the Milky Way mentioned above have different values of the parameters (ℓ and η). This is because these two galaxies have different mass distributions (See the

Table 1. The fitting parameters for the lens model of this paper in the mass unit of $10^9 M_\odot$ and the length unit of 1 arcsec.

ℓ	η	α	β	q	M	χ^2
1.5564×10^{-4}	2.8658	−0.8949	−0.5352	3.7633	5.0279×10^3	1.1964

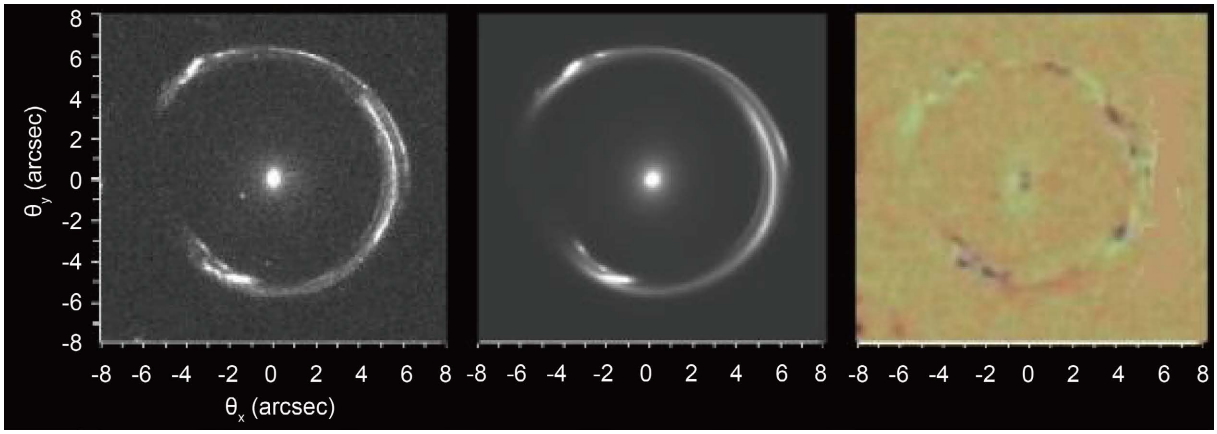

Figure 6. Fitting results based on the lens model (10). *Left*: Observed image of the Cosmic Horseshoe, with north up and east left. Middle: Fitting image; *Right*: The residuals obtained by subtracting the fitted image from the observed image.

hypothesis about ℓ and η in the analysis (1) in Section 2).

In Table 1, M contains the baryon matter mass of $1.1040\times10^{11} M_\odot$ and the dark matter mass of $4.9175\times10^{12} M_\odot$. These three masses are calculated by integrating the total surface mass density of the lens, the surface mass density of baryon matter and the surface mass density of dark matter in (11) within the Einstein ring on the lens plane, respectively.

To sum up, EVPF, which is a self-acting mixture containing various virtual particles excited by the gravitational field of ordinary matter, can show the properties and phenomena of dark matter and may become a candidate for dark matter. This kind of dark matter can be called "virtual particle dark matter" (VPDM).

So, what is the essence of ordinary matter? As a comparison with dark matter, ordinary matter should be regarded as the real particle field which can be directly detected by instruments, while dark matter may never be directly detected by instruments because it may be virtual particles.

3. Improvement of Kinetic Equations

Considering the impact of Equation (1), cosmological hydrodynamic equations and cosmic perturbation equations need to be improved.

3.1. Improvement of Hydrodynamic Equations

For an evolutionary gravitational system, due to the continuous change of mass distribution, the system has different mass distributions at different moments. According to the assumption about ℓ and η in the analysis (1) in Section 2, ℓ and η also take different values at different moments, *i.e.* they are the functions of time. So, (1) can be written as

$$\rho_D = \ell(t)\left(E_{LM}\right)^{\eta(t)} + \rho_{vac} \tag{12}$$

Equation (12) is in the usual coordinate system with coordinate $\vec{r}$,whereas the cosmological hydrodynamic equations and cosmic perturbation equations are usually in the comoving coordinate system. So, it is necessary to transform (12) into the comoving coordinate system.

Let Φ_{LM} represent the gravitational potential of ordinary matter, then (12) can be deformed into

$$\begin{aligned}\rho_D &= \ell(t)\left[E_{LM}^2\right]^{\eta(t)/2} + \rho_{vac} = \ell(t)\left[\vec{E}_{LM}\cdot\vec{E}_{LM}\right]^{\eta(t)/2} + \rho_{vac} \\ &= \ell(t)\left[\nabla\Phi_{LM}\cdot\nabla\Phi_{LM}\right]^{\eta(t)/2} + \rho_{vac} \approx \ell(t)\left[\nabla\Phi_{LM}\cdot\nabla\Phi_{LM}\right]^{\eta(t)/2}.\end{aligned} \tag{13}$$

(13) is expressed in the usual coordinates $\vec{r}$.

Using Equation (7.7) in reference [16]

$$\phi = \Phi + a\ddot{a}x^2/2$$

(Here ϕ is the newly defined gravitational potential in the comoving coordinate system in reference [16] based on the canonical transformation of the Lagrangian of the system) and Equation (9.34) in reference [17]

$$\ddot{a} = -4\pi Ga\left(\bar{\rho} + 3\bar{P}\right)/3,$$

(Here Equation (9.34) results from the $(\mu\nu) = (00)$ component of Einstein gravitational field equation describing cosmic background in reference [17] when the cosmological constant Λ is ignored)

(13) is changed into

$$\begin{aligned}\rho_D = \ell(t)a^{-\eta(t)}&\left[\left(\nabla\phi_{LM} + 4\pi Ga^2\left(\bar{\rho}_{LM} + 3\bar{P}_{LM}\right)\vec{x}/3\right)\right. \\ &\left.\cdot\left(\nabla\phi_{LM} + 4\pi Ga^2\left(\bar{\rho}_{LM} + 3\bar{P}_{LM}\right)\vec{x}/3\right)\right]^{\eta(t)/2}\end{aligned} \tag{14}$$

where $\vec{x}$ is the comoving coordinate, $x^2 = |\vec{x}|^2 = x_1^2 + x_2^2 + x_3^2$. ϕ, $\bar{\rho}$, $\bar{P}$ and a are the newly defined gravitational potential, cosmic background density, cosmic background pressure and cosmic scale factor, respectively. The coordinate transformation $\vec{x} = \vec{r}/a$ is used in gradient operations.

(14) is expressed in the comoving coordinates $\vec{x}$.

As a universal relationship between dark matter and the gravitational field of ordinary matter, (14) should be added as a constraint to the kinetic equations describing the cosmic structures such as galaxies, galaxy clusters, and the large-scale structures of the universe etc. Thus, the improved cosmological hydrodynamic equations are

$$\text{Euler's equation}\quad \frac{\partial\vec{v}_1}{\partial t} + \frac{1}{a}\left(\vec{v}_1\cdot\nabla\right)\vec{v}_1 + \frac{\dot{a}}{a}\vec{v}_1 = -\frac{1}{\rho_1 a}\nabla P_1 - \frac{1}{a}\nabla\left(\phi_1 + \phi_2\right), \tag{15}$$

$$\text{continuity equation}\quad \frac{\partial\rho_1}{\partial t} + \frac{\dot{a}}{a}\rho_1 + \frac{1}{a}\nabla\cdot\left(\rho_1\vec{v}_1\right) = 0, \tag{16}$$

first law of thermodynamics

$$\frac{\partial\left(\rho_1 u_1\right)}{\partial t} + \frac{1}{a}\vec{v}_1\cdot\nabla\left(\rho_1 u_1\right) = -\left(\rho_1 u_1 + P_1\right)\left(\frac{1}{a}\nabla\cdot\vec{v}_1 + 3\frac{\dot{a}}{a}\right), \tag{17}$$

$$\text{Euler's equation} \quad \frac{\partial \vec{v}_2}{\partial t}+\frac{1}{a}\left(\vec{v}_2\cdot\nabla\right)\vec{v}_2+\frac{\dot{a}}{a}\vec{v}_2=-\frac{1}{a}\nabla\left(\phi_1+\phi_2\right), \tag{18}$$

$$\text{continuity equation} \quad \frac{\partial \rho_2}{\partial t}+\frac{\dot{a}}{a}\rho_2+\frac{1}{a}\nabla\cdot\left(\rho_2\vec{v}_2\right)=0, \tag{19}$$

first law of thermodynamics

$$\frac{\partial\left(\rho_2 u_2\right)}{\partial t}+\frac{1}{a}\vec{v}_2\cdot\nabla\left(\rho_2 u_2\right)=-\left(\rho_2 u_2\right)\left(\frac{1}{a}\nabla\cdot\vec{v}_2+3\frac{\dot{a}}{a}\right), \tag{20}$$

$$\text{Gravitational equation} \quad \nabla^2\phi_1=4\pi G a^2\left[\left(\rho_1-\bar{\rho}_1\right)+3\left(P_1-\bar{P}_1\right)\right], \tag{21}$$

$$\text{Gravitational equation} \quad \nabla^2\phi_2=4\pi G a^2\left(\rho_2-\bar{\rho}_2\right), \tag{22}$$

$$\begin{aligned}\text{constraint} \quad \rho_2=\ell(t)a^{-\eta(t)}\Big[&\left(\nabla\phi_1+4\pi G a^2\left(\bar{\rho}_1+3\bar{P}_1\right)\vec{x}/3\right)\\ &\cdot\left(\nabla\phi_1+4\pi G a^2\left(\bar{\rho}_1+3\bar{P}_1\right)\vec{x}/3\right)\Big]^{\eta(t)/2}.\end{aligned} \tag{23}$$

Here two subscripts 1 and 2 represent baryon matter and dark matter, respectively. The gravitational equations of baryon matter and dark matter are written separately in order to write the constraint condition.

At large scale, $\bar{\rho}_1 \ll \bar{\rho}_2$, the contribution of baryon matter can be ignored. In this case, (15), (16), (17), (21) and (23) can be omitted, only leaving (18), (19), (20) and (22) considered and simultaneously letting $\phi_1=0$. This is the so-called "dark-matter-only simulation". Whereas at small scale, in the comparison of average density, $\bar{\rho}_1 \sim \bar{\rho}_2$, the contribution of baryon matter cannot be ignored, and (15)-(23) all need to be taken into account. That is to say, at large scale, we can only consider dark matter. But, at small scale, both dark matter and baryonic matter must be simultaneously taken into account in the simulation. This is why the usual "dark-matter-only simulation" can well conform to the large-scale observations of the universe, but it faces challenges at small scale.

However, even if baryon matter and dark matter are considered at the same time, the problem of missing satellite galaxies has not been well solved [18] [19] [20]. What should we do? We still have a constraint condition that hasn't been applied. Considering baryon matter and dark matter at the same time, and adding the constraint (23), the above improved equations are expected to solve the satellite galaxies' problem.

But, there is still a cusp-core problem. How to solve it? When the self-interaction of EVPF is considered (After all, according to the assumption ② in the analysis (1) in Section 2, in the case of strong gravitational field (such as galactic center), EVPF's self-interaction is also not weak), it becomes viscous fluid, and the above kinetic equations need to be further modified. After considering viscosity and constraint, the improved equations are expected to solve the cusp-core problem.

The improvement of the hydrodynamic equations provides a new method for solving the small-scale challenges faced by LCDM.

3.2. Improvement of Cosmic Perturbation Equations

As a universal relationship between dark matter and the gravitational field of ordinary matter, (14) also should be added as a constraint to the equations describing cosmic perturbations. Thus, the improved cosmic perturbation equations for the gravitational field and the four cosmic components (baryon, photon, neutrino, dark matter) during the baryon-photon Thomson scattering in the early universe, in the comoving coordinates, are listed below.

3.2.1. Gravitational Field Equations

According to the Equations (12.84) and (12.88) in reference [17]), the gravitational field equations for cosmic perturbations can be written as

$$
\begin{aligned}
&-4\pi G\left(\delta\rho_B+2\delta\rho_\gamma/3+2\delta\rho_\nu/3\right)\\
&=\left(-\frac{1}{2}\partial_t^2-3H\partial_t+\frac{1}{2a^2}\nabla^2\right)\left(A_O+2H\left(2\delta u_\gamma^{(S)}+\delta u_\nu^{(S)}\right)\right)\\
&\quad+\left(\frac{1}{2}H\partial_t+2H^2+\frac{\ddot{a}}{a}\right)\left(E_O+2\left(2\delta\dot{u}_\gamma^{(S)}+\delta\dot{u}_\nu^{(S)}\right)\right)\\
&\quad+\frac{H}{a}\nabla^2\left(F_O-\frac{a}{2}\dot{B}_O-\frac{1}{a}\left(2\delta u_\gamma^{(S)}+\delta u_\nu^{(S)}\right)\right),\\
&-4\pi G\delta\rho_D=\left(-\frac{1}{2}\partial_t^2-3H\partial_t+\frac{1}{2a^2}\nabla^2\right)A_D-\left(\frac{1}{2}H\partial_t+2H^2+\frac{\ddot{a}}{a}\right)E_O\\
&\qquad-\frac{H}{a}\nabla^2\left(F_O+\frac{a}{2}\dot{B}_D\right),\\
&\partial_j\partial_k\left[\left(\left(A_O+A_D\right)+2H\left(2\delta u_\gamma^{(S)}+\delta u_\nu^{(S)}\right)\right)+2\left(2\delta\dot{u}_\gamma^{(S)}+\delta\dot{u}_\nu^{(S)}\right)\right.\\
&\left.+2a\left(\partial_t+2H\right)\left(-\frac{a}{2}\left(\dot{B}_O+\dot{B}_D\right)-\frac{1}{a}\left(2\delta u_\gamma^{(S)}+\delta u_\nu^{(S)}\right)\right)\right]=0,\\
&\partial_j\left(\partial_t\left(\left(A_O+A_D\right)+2H\left(2\delta u_\gamma^{(S)}+\delta u_\nu^{(S)}\right)\right)-2H\left(2\delta\dot{u}_\gamma^{(S)}+\delta\dot{u}_\nu^{(S)}\right)\right)=0,\\
&-4\pi G\left(\delta\rho_B+2\delta\rho_\gamma+2\delta\rho_\nu\right)\\
&=\left(\frac{3}{2}\partial_t^2+3H\partial_t\right)\left(A_O+2H\left(2\delta u_\gamma^{(S)}+\delta u_\nu^{(S)}\right)\right)\\
&\quad-\left(\frac{3}{2}H\partial_t+3\frac{\ddot{a}}{a}+\frac{1}{2a^2}\nabla^2\right)\left(E_O+2\left(2\delta\dot{u}_\gamma^{(S)}+\delta\dot{u}_\nu^{(S)}\right)\right)\\
&\quad-\frac{1}{a}\left(\partial_t+H\right)\nabla^2\left(F_O-\frac{a}{2}\dot{B}_O-\frac{1}{a}\left(2\delta u_\gamma^{(S)}+\delta u_\nu^{(S)}\right)\right),\\
&-4\pi G\delta\rho_D=\left(\frac{3}{2}\partial_t^2+3H\partial_t\right)A_D+\left(\frac{3}{2}H\partial_t+3\frac{\ddot{a}}{a}+\frac{1}{2a^2}\nabla^2\right)E_O\\
&\qquad+\frac{1}{a}\left(\partial_t+H\right)\nabla^2\left(F_O+\frac{a}{2}\dot{B}_D\right).
\end{aligned}
\tag{24}
$$

Here, regarding the derivation of (24), the following several points need to be explained:

First, five subscripts B, γ, ν, O and D represent baryon, photon, neutrino,

ordinary matter (Here ordinary matter refers to baryon, photon and neutrino) and dark matter, respectively.

Second, $\delta\rho$ and $\delta u^{(S)}$ represent the mass density perturbation and velocity potential perturbation, respectively.

Third, A_O, B_O, E_O, F_O and A_D, B_D are the components of metric perturbations contributed by ordinary matter and dark matter respectively, coming from the metric perturbation [17]

$$h_{\mu\nu} = \begin{pmatrix} h_{00} & h_{0j} \\ h_{j0}\left(=h_{0j}\right) & h_{jk} \end{pmatrix} = \begin{pmatrix} -E & a\left(\partial_j F + G_j\right) \\ h_{0j} & a^2\left(A\delta_{jk} + \partial_j\partial_k B + \partial_j C_k + \partial_k C_j + D_{jk}\right) \end{pmatrix}, \quad (j,k=1,2,3)$$

where the Helmholtz decomposition of h_{0j} and h_{jk} is used. $A = A_O + A_D$, $B = B_O + B_D$, $C_j = C_{jO} + C_{jD}$, $D_{jk} = D_{jkO} + D_{jkD}$, $E = E_O + E_D$, $F = F_O + F_D$, $G_j = G_{jO} + G_{jD}$.

Fourth, for the description and explanation of the CMB anisotropy only the scalar functions are important. So the expressions involving only scalar functions A, B, E, F are considered in the derivation of (24), without the consideration of the vector C_j, G_j and the tensor D_{jk}.

Fifth, the derivation uses the synchronous gauge which is defined by setting [17]

$$E + 2\dot{\varepsilon}_0 = 0, \quad F - \frac{1}{a}\left[\varepsilon_0 + a^2\partial_t\left(\frac{\varepsilon^{(S)}}{a^2}\right)\right] = 0.$$

Where ε_0 and $\varepsilon^{(S)}$ origin from rewriting the infinitesimal coordinate shift 4-vector $\varepsilon_\mu\left(\vec{x},t\right)$ as follows [17]:

$$\varepsilon_\mu \equiv \left(\varepsilon_0, \varepsilon_j\right), \quad \varepsilon_j \equiv \partial_j\varepsilon^{(S)} + \varepsilon_j^{(V)}, \quad \partial_j\varepsilon_j^{(V)} = 0.$$

ε_μ can achieve the following coordinate transformation [17]

$$x_\mu \to x'_\mu = x_\mu + \varepsilon_\mu\left(x\right).$$

In the derivation of (24), letting $E = 0, F = 0$ (*i.e.* $E_D = -E_O$ and $F_D = -F_O$) are used.

Sixth, the gravitational field equations of ordinary matter and dark matter are written separately (See the first two equations and the last two equations of Equation (24)) in order to write the constraint condition below.

Seventh, the approximations $\pi^{(S)} = 0$, $\delta u_D^{(S)} = 0$, $\delta u_B^{(S)} = \delta u_\gamma^{(S)}$, $\delta P_B = \delta P_D = \overline{P}_B = \overline{P}_D = 0$, $\overline{P}_\gamma = \overline{\rho}_\gamma/3$, $\delta P_\gamma = \delta\rho_\gamma/3$, $\overline{P}_\nu = \overline{\rho}_\nu/3$, $\delta P_\nu = \delta\rho_\nu/3$ in the section 12.9.1 of reference [17] are used in the derivation of (24). These approximations will also be used below.

3.2.2. Conservation Equations of Energy

Each of the four cosmic components has its energy density evolution equation. According to the first equation of Equation (12.108) in reference [17], there are four conservation equations of energy:

$$\begin{aligned}
&\delta\dot{\rho}_D + 3H\delta\rho_D + \frac{1}{2}\bar{\rho}_D\left(3\left(\dot{A}_O + \dot{A}_D\right) + \nabla^2\left(\dot{B}_O + \dot{B}_D\right)\right) = 0,\\
&\delta\dot{\rho}_B + 3H\delta\rho_B + \frac{1}{a^2}\bar{\rho}_B\nabla^2\delta u_\gamma^{(S)} + \frac{1}{2}\bar{\rho}_B\left(3\left(\dot{A}_O + \dot{A}_D\right) + \nabla^2\left(\dot{B}_O + \dot{B}_D\right)\right) = 0,\\
&\delta\dot{\rho}_\gamma + 4H\delta\rho_\gamma + \frac{4}{3a^2}\bar{\rho}_\gamma\nabla^2\delta u_\gamma^{(S)} + \frac{2}{3}\bar{\rho}_\gamma\left(3\left(\dot{A}_O + \dot{A}_D\right) + \nabla^2\left(\dot{B}_O + \dot{B}_D\right)\right) = 0,\\
&\delta\dot{\rho}_\nu + 4H\delta\rho_\nu + \frac{4}{3a^2}\bar{\rho}_\nu\nabla^2\delta u_\nu^{(S)} + \frac{2}{3}\bar{\rho}_\nu\left(3\left(\dot{A}_O + \dot{A}_D\right) + \nabla^2\left(\dot{B}_O + \dot{B}_D\right)\right) = 0.
\end{aligned} \tag{25}$$

3.2.3. Conservation Equations of Momentum

According to the section 12.9.2.1.3 of reference [17], the momentum of the cold dark matter is neglected. The baryonic matter and photon are coupled in their momenta so they enter jointly in the momentum conservation equation. The neutrino has its separate momentum conservation equation. From the second expression of Equation (12.108) in reference [17], we can obtain the equations for the perturbation functions of the velocity potentials:

$$\begin{aligned}
&\partial_j\left(\frac{1}{3}\delta\rho_\gamma + \left(\partial_t + 3H\right)\left(\left(\bar{\rho}_B + \frac{4}{3}\bar{\rho}_\gamma\right)\delta u_\gamma^{(S)}\right)\right) = 0,\\
&\partial_j\left(\frac{1}{3}\delta\rho_\nu + \left(\partial_t + 3H\right)\left(\frac{4}{3}\bar{\rho}_\nu\delta u_\nu^{(S)}\right)\right) = 0;
\end{aligned} \tag{26}$$

3.2.4. The Constraint about the Relationship between Dark Matter Density and Gravity

According to (14), the constraint condition for the cosmic perturbation equations is

$$\begin{aligned}
\delta\rho_D = \ell(t)a^{-\eta(t)}&\left[\left(\nabla\left(\frac{E_O}{2}\right) + \frac{4\pi G}{3}a^2\left(\bar{\rho}_B + 2\bar{\rho}_\gamma + 2\bar{\rho}_\nu\right)\vec{x}\right)\right.\\
&\left.\cdot\left(\nabla\left(\frac{E_O}{2}\right) + \frac{4\pi G}{3}a^2\left(\bar{\rho}_B + 2\bar{\rho}_\gamma + 2\bar{\rho}_\nu\right)\vec{x}\right)\right]^{\eta(t)/2} - \bar{\rho}_D.
\end{aligned} \tag{27}$$

where $E_O = 2\phi_O$, ϕ_O is referred to as the Newtonian potential of ordinary matter.

From the point of view of VPDM, since both dark matter and ordinary matter are included in cosmic perturbation equations, then as a constraint condition to describe the relationship between dark matter and the gravitational field of ordinary matter, (27) must be added to cosmic perturbation equations. However, there is usually no such constraint in the calculations of cosmic perturbations. This may be the reason for the Hubble constant crisis. If incorporating the constraint (27), the improved equations are expected to solve this crisis that troubles the academic community.

It can be predicted that due to the impact of (27), under the condition of fitting the observed angular power spectrum with the same accuracy as the usual LCDM, the improved LCDM will result in a Hubble constant value different from current fit value (67.4 ± 0.5 km/(s·Mpc) [21]) and a ratio different from current fit ratio (4.9%:26.8%:68.3% [17]) about the energy densities of ordinary

matter, dark matter and dark energy.

The improvement of the cosmic perturbation equations offers a new approach to solving the Hubble constant crisis encountered by LCDM.

4. Conclusion

This article proposes the hypothesis of VPDM, arguing that EVPF can show the properties and phenomena of dark matter and may become the essence or candidate of dark matter. Different from popular particle dark matter models, VPDM is a dark matter mechanism that does not exceed the particle physics standard model. But as virtual particle, VPDM will never be directly detected by instruments. Considering the constraint relationship between dark matter density and gravitational field of ordinary matter, the hydrodynamic equations and cosmic perturbation equations describing cosmic matter are improved. This offers a unified solution to the small-scale difficulties and Hubble constant crisis, probably having an impact on developing and perfecting LCDM model and solving its self-consistency problem. The next work is to do factual compution to test the solution in this article. Here, the author strongly recommends that scientists use these improved dynamic equations to recalculate Hubble constant and cosmic small scale evolution to test these equations. In addition to the small-scale difficulties and Hubble constant crisis, whether the improved LCDM can solve the other challenges in a package is a problem to be further studied.

If dark matter is regarded as the excited virtual particle field, ordinary matter is real particle field, whereas dark energy is the ground-state virtual particle field (vacuum). That is to say, dark matter and dark energy are homologous, coming both from the virtual particle field of the universe and being the different states of the same virtual particle field.

Conflicts of Interest

The author declares no conflicts of interest regarding the publication of this paper.

References

[1] Perivolaropoulos, L. and Skara, F. (2022) *New Astronomy Reviews*, **95**, 101659-101764. https://doi.org/10.1016/j.newar.2022.101659

[2] Abdalla, E., Abellán, G.F., Aboubrahim, A., *et al.* (2022) *Journal of High Energy Astrophysics*, **34**, 49-211.

[3] Vagnozzi, S. (2023) *Universe*, **9**, 393.

[4] Chang, Z., Chen, S.X., Wen, H.B., *et al.* (2005) *International Journal of Modern Physics A*, **20**, 2157-2172. https://doi.org/10.1142/S0217751X05020720

[5] Vikram, V., *et al.* (2015) Wide-Field Lensing Mass Maps from DES Science Verification Data.

[6] Binney, J. and McMillan, P. (2011) *Monthly Notices of the Royal Astronomical Society*, **413**, 1889-1898. https://doi.org/10.1111/j.1365-2966.2011.18268.x

[7] Esko, G. and Chris, F. (2010) *Monthly Notices of the Royal Astronomical Society*,

405, 545-552.

[8] Zhou, Y., Li, X.Y., Huang, Y., Zhang, H.W., *et al.* (2023) *The Astrophysical Journal*, **946**, 73-87. https://doi.org/10.3847/1538-4357/acadd9

[9] Jing, Y.P. and Suto, Y. (2002) *The Astrophysical Journal*, **574**, 538-553. https://doi.org/10.1086/341065

[10] Hayashi, E., Navarro, J.F. and Springel, V. (2007) *Monthly Notices of the Royal Astronomical Society*, **377**, 50-62.

[11] Pato, M. and Iocco, F. (2015) *The Astrophysical Journal Letters*, **803**, L3. https://doi.org/10.1088/2041-8205/803/1/L3

[12] Massimo, P., Paolo, S. and Fulvio, S. (1996) *MNRAS*, **281**, 27-48. https://doi.org/10.1093/mnras/278.1.27

[13] Dye, S., Evans, N.W., *et al.* (2010) *Monthly Notices of the Royal Astronomical Society*, **388**, 384-392. https://doi.org/10.1111/j.1365-2966.2008.13401.x

[14] Bellagamba, F., Tessore, N. and Metcalf, R.B. (2017) *Monthly Notices of the Royal Astronomical Society*, **464**, 4823-4834. https://doi.org/10.1093/mnras/stw2726

[15] John, E.K.A., Richard, N.H.B. and Felix, S.B. (2012) *Proceedings of SPIE—The International Society for Optical Engineering*, **8127**, 777-785.

[16] Peebles, P.J.E. (1980) The Large Scale Structure of the Universe. Princeton University Press, Princeton, 435 p.

[17] Young, B.-L. (2017) *Frontiers in Physics*, **12**, Article ID: 121201. https://doi.org/10.1007/s11467-017-0680-z

[18] Wetzel, A.R., *et al.* (2016) *The Astrophysical Journal*, **827**, 23. https://doi.org/10.3847/0004-637X/827/1/23

[19] Kelley, T., *et al.* (2019) *MNRAS*, **487**, 4409-4423. https://doi.org/10.1093/mnras/stz1553

[20] Drlica-Wagner, A., *et al.* (2020) *The Astrophysical Journal*, **893**, 47. https://doi.org/10.3847/1538-4357/ab7eb9

[21] Aghanim, N., *et al.* (2020) *A&A*, **641**, A6.